Nucleation in a slit pore

V. Talanquer
Department of Chemistry, University of Arizona, Tucson, Arizona 85721

D. W. Oxtoby[a)]
The James Franck Institute, The University of Chicago, 5640 S. Ellis Ave., Chicago, Illinois 60637

(Received 7 August 2000; accepted 16 November 2000)

We have employed density functional theory in statistical mechanics to study the nucleation of the gas–liquid transition inside a slit pore. This is the simplest kind of pore, in which a fluid is confined between two infinite and identical planar surfaces. Equilibrium capillary condensation in such systems has been studied in the past. Here, we explore the kinetics of nucleation of the new phase and show that the critical nucleus can either be attached to one of the planes or can bridge the two planes, depending on the conditions of the experiment. We show that the macroscopic capillarity approximation is not quantitatively accurate, but can provide a useful qualitative picture provided that the line tension is incorporated. Comparisons are made with recent simulations of phase transitions in slit pores. © *2001 American Institute of Physics.* [DOI: 10.1063/1.1339223]

I. INTRODUCTION

The properties of fluids in porous media are important to a variety of fields. Oil and water in rocks and sand are a familiar geological example; recent applications rely on the transport of chemicals through porous catalysts and the production of porous materials with particular electronic or structural properties. One way in which such materials are characterized is through the investigation of the phase transitions that fluids undergo inside their pores.

Capillary condensation in nanoporous materials shows a range of phenomena much broader than is seen in the bulk gas–liquid transition. The existence of nanometer length scales in such pores leads to competition between fluid–fluid and fluid–substrate forces that gives rise to entirely new phase behavior in which wetting and drying play a central role.[1] Most of the work in this area to date has emphasized equilibrium aspects of the phase transitions.

The existence of large-scale hysteresis in capillary condensation suggests, however, that dynamics is important as well. An understanding of phase transition dynamics at the simplest, single-pore, level is a necessary prerequisite for a study of the more complex behavior that depends on pore topology and connectivity. Nucleation of first-order phase transitions inside pores is a little-studied problem that is nonetheless a key ingredient for a full theory of fluids in pores. Recently, this problem has attracted some interest, with an initial focus on slit pores in which fluids are confined between a pair of infinite flat plates. Yasuoka *et al.*[2] used molecular dynamics techniques to study condensation in relatively thick slit pores, whereas Bolhuis and Chandler[3] used molecular dynamics and Monte Carlo methods to study the drying transition in narrow pores. Restagno *et al.*[4] applied a macroscopic approach (employing the capillarity approximation) to predict the behavior of critical nuclei in both two and three dimensions, and then carried out a time-dependent Landau–Ginzburg simulation of condensation in two dimensions.

In this paper, we apply the methods of density functional theory to study the nucleation of the gas–liquid transition inside a slit pore. In earlier work, we have demonstrated the usefulness of this approximate statistical mechanical theory for studying both homogeneous nucleation[5] and heterogeneous nucleation on planar substrates.[6] We show in the present paper that there is a crossover from a critical nucleus attached to one of the planar surfaces (at large enough pore widths) to one that bridges the two surfaces (for narrow enough pores).

The outline of the paper is as follows. In Sec. II we describe the density functional employed and apply it to the problem of a slit pore. The equilibrium phase diagram of a fluid between pores (including capillary condensation) is presented in Sec. III. Section IV then turns to the question of heterogeneous nucleation in a pore, while Sec. V explores the same question from the macroscopic point of view of the capillarity approximation. Section VI concludes with a discussion of further steps to be explored in the future.

II. DENSITY FUNCTIONAL THEORY

In order to obtain information about capillary coexistence and heterogeneous nucleation of a fluid in a slit pore, a theory for confined inhomogeneous fluids is required. For that purpose, we consider a fluid confined by two parallel adsorbing walls of area A_s, unbounded in the two directions parallel to the plates and held in equilibrium at a separation L by a force applied externally. The grand potential of the system Ω is assumed to be a functional of the local density $\rho(\mathbf{r})$ and to have the form[7,8]

$$\Omega[\rho(\mathbf{r})]=\int d\mathbf{r}[f[\rho(\mathbf{r})]-\mu\rho(\mathbf{r})]+\frac{K}{2}\int d\mathbf{r}[\nabla\rho(\mathbf{r})]^2+\int_{A_s}\Phi[\rho(\mathbf{r})]d\mathbf{a}, \tag{1}$$

a)Electronic mail: d-oxtoby@uchicago.edu

where $f[\rho(r)]$ is the local Helmholtz free-energy density, and where the square-gradient term accounts for the free-energy cost associated with spatial variations of the density. For a van der Waals fluid, the local Helmholtz free energy density is given by[9]

$$f[\rho]=kT\rho[\ln\rho-1-\ln(1-b\rho)]-a\rho^2, \tag{2}$$

where k is Boltzmann's constant, T is the absolute temperature, and a and b are phenomenological parameters. The latter parameters, a and b, are chosen in order to include, respectively, the effect of long-range attractive forces between particles and the molecular size.

The last term in the grand potential functional described by Eq. (1), $\Phi[\rho(\mathbf{r})]$, is introduced to take into account contributions due to fluid–solid interactions. We further assume that the interactions between the fluid and the confining walls are sufficiently short ranged that their contributions to the free energy only depend on the densities at contact ρ_o and ρ_L[8]

$$\Phi[\rho_o,\rho_L]=-h_o\rho_o-\tfrac{1}{2}g_o\rho_o^2-h_L\rho_L-\tfrac{1}{2}g_L\rho_L^2, \tag{3}$$

where h_o and h_L represent the surface fields and g_o and g_L account for the possible enhancement of molecular interactions at the corresponding substrates at $z=0$ and $z=L$, respectively.

In this work we consider the limit in which the area of each plate A_s goes to infinity, but the confined system is still in contact with a reservoir of fluid with the same temperature T and chemical potential μ. The properties of the surrounding van der Waals fluid are hence well known: the fluid exhibits two-phase coexistence between a liquid and a vapor at temperatures lower than the critical value $kT_c=8a/27b$.

The properties of equilibrium inhomogeneous states in the system can be obtained by minimizing the grand potential functional in Eq. (1) with respect to $\rho(\mathbf{r})$. The corresponding density profiles satisfy the associated Euler–Lagrange equation[10]

$$\frac{\delta\Omega[\rho(\mathbf{r})]}{\delta\rho(\mathbf{r})}=\frac{df[\rho(\mathbf{r})]}{d\rho(\mathbf{r})}-\mu-K\nabla^2\rho(\mathbf{r})=0, \tag{4}$$

that can be solved under appropriate boundary conditions. For any given interface of area A, the associated surface tension γ is given by the grand potential excess per unit area

$$A\gamma=\Omega[\rho(\mathbf{r})]-\Omega_u[\rho], \tag{5}$$

where $\Omega[\rho(\mathbf{r})]$ is the grand potential of the equilibrium density profile for the inhomogeneous system, and $\Omega_u[\rho]=-PV$ is the grand potential of the bulk uniform fluid in the reservoir (with pressure P) at the same temperature and chemical potential.

For the reservoir fluid, Eq. (4) can be solved using standard numerical techniques to generate the density profiles for the liquid–gas interface at a given temperature. The interfacial tension for this interface γ_{lg} is then given by Eq. (5) with $\Omega_u/V=-P_{\mathrm{sat}}$, the bulk saturation pressure. For the particular case of the fluid confined between two planar interfaces perpendicular to the z axis and located at $z=0$ and $z=L$, one can integrate Eq. (4) to obtain[11,12]

$$\frac{K}{2}(d\rho(z)/dz)^2=\Delta\omega(\rho(z))-\Delta\omega(\rho_m), \tag{6}$$

where

$$\Delta\omega(\rho(z))=\omega(\rho(z))-\Omega_u/V=f(\rho(z))-\mu\rho(z)+P, \tag{7}$$

and $\Delta\omega(\rho_m)$ is an integration constant. In the limit of infinite wall separation, $\Delta\omega(\rho_m)$ vanishes, but in general, it corresponds to the value of $\Delta\omega(\rho(z))$ at a point where the slope of the profile is zero. In the special case of symmetrical walls ($h_o=h_L=h$, $g_o=g_L=g$), $\rho_m=\rho(L/2)$. It can be shown that the absolute value of $\Delta\omega(\rho_m)$ is a direct measure of the magnitude of the solvation force between the two walls of the capillary.[12]

Equation (6) can be integrated again to generate an implicit expression for the density profile $\rho(z)$ as a function of the separation L

$$\left(\frac{2}{K}\right)^{1/2}L=\left|\int_{\rho_o}^{\rho_m}(\Delta\omega(\rho)-\Delta\omega(\rho_m))^{-1/2}\right|+\left|\int_{\rho_m}^{\rho_L}(\Delta\omega(\rho)-\Delta\omega(\rho_m))^{-1/2}\right|, \tag{8}$$

where ρ_o and ρ_L are determined, respectively, by

$$(d\rho/dz)_{z=0}=\mathrm{sign}(\rho_m-\rho_o)\left[\frac{2(\Delta\omega(\rho_o)-\Delta\omega(\rho_m))}{K}\right]^{1/2}$$

$$(d\rho/dz)_{z=L}=\mathrm{sign}(\rho_L-\rho_m)\left[\frac{2(\Delta\omega(\rho_L)-\Delta\omega(\rho_m))}{K}\right]^{1/2}, \tag{9}$$

and the boundary conditions

$$K(d\rho/dz)_{z=0}=-h_o-g_o\rho_o,$$

$$K(d\rho/dz)_{z=L}=h_L+g_L\rho_L. \tag{10}$$

Equations (6) through (10) can also be used to calculate the properties of any bulk phase in contact with a flat wall at $z=0$. It is only necessary to consider the case $h_L=g_L=0$ in the limit $L\to\infty$.[13] The corresponding surface tensions for the coexisting bulk liquid and bulk gas in contact with the wall (γ_{sl} and γ_{sg}, respectively), can then be used together with γ_{lg} and Young's equation

$$\gamma_{sv}-\gamma_{sl}=\gamma_{lg}\cos\theta_o, \tag{11}$$

to calculate the bulk contact angle θ_o at a single wall as predicted by the model for given values of h_o, g_o, and T.

III. CAPILLARY COEXISTENCE

For the fluid confined in the capillary, the condensation of a liquid-like phase can occur at values of the external pressure P that are either higher or lower than P_{sat}, depending on the nature and strength of the interactions of the fluid particles with the confining walls.[14,15] In either case, phase coexistence between two inhomogeneous phases adsorbed in the capillary is achieved when their corresponding excess grand potentials, as defined in Eq. (5), are equal. In the limit $L\to\infty$, the phase equilibria of the fluid should be determined

by macroscopic considerations. In a first approximation, if we think of a slit pore of volume $V=AL$ immersed in a gas at pressure P, we can write[16]

$$\Delta\Omega_g=\gamma_{sg}A, \tag{12a}$$

$$\Delta\Omega_l=-(P_l-P)V+\gamma_{sl}A, \tag{12b}$$

for the adsorbed gas and the adsorbed liquid phases, respectively, in the capillary. A phase transition from one configuration to the other will occur when $\Delta\Omega_g=\Delta\Omega_l$, or when the pressure in the reservoir satisfies

$$P_l-P=-(\gamma_{sg}-\gamma_{sl})A/V=-2\gamma_{lg}\cos\theta_o/L, \tag{13}$$

where we have introduced Young's equation [Eq. (11)]. If we further assume that the liquid is incompressible and the gas is close to ideal, $\Delta P=P_l-P$ can be approximated by

$$\Delta P\approx\rho_l kT\ln(P/P_{\text{sat}})=\rho_l kT\ln(S), \tag{14}$$

where ρ_l is the density of the liquid phase and $S=P/P_{\text{sat}}$ is the bulk supersaturation. By substituting Eq. (14) in Eq. (13) we derive the Kelvin equation for the pressure at which condensation occurs inside the capillary

$$\rho_l kT\ln(S)=-2\gamma_{lg}\cos\theta_o/L. \tag{15}$$

As we can see, the Kelvin equation predicts that capillary condensation will occur at supersaturations $S\leqslant 1$ for fluids with a bulk contact angle $0\leqslant\theta_o\leqslant\pi/2$, and in supersaturated vapors ($S>1$) for systems with higher contact angles. In either case, the deviations from the condition of coexistence in the reservoir become larger in the narrower pores. For smaller values of L or under wetting conditions, however, the former macroscopic arguments do not apply and deviations from the predictions of Eq. (15) occur.

We have explored the conditions for capillary coexistence in a slit pore with symmetrical walls ($h_o=h_L=h$, $g_o=g_L=g$) as a function of the width L as predicted by our model. The location of the binodal and spinodals for different values of L is a useful guide in analyzing the process of nucleation inside the capillary. We have set the dimensionless constant $K/(kT_c b^{5/3})=4.0$ in all our calculations; this value leads to reasonable estimates of the surface tension for real liquids at several temperatures. The value of the surface enhancement field g has also been chosen to try to mimic the behavior of real fluids; in particular we set $g=-K/b$, following Nakanishi and Fisher.[11] We will discuss the effect of different values of the surface field h on the behavior of the system, but our analysis will be restricted to values of h and T that lead to partial wetting ($0<\theta_o\leqslant\pi/2$) or partial drying ($\pi/2<\theta_o<\pi$). All our numerical results are expressed in reduced units, with $b^{1/3}$ as the unit of length and $kT_c=27a/8b$ as the unit of energy ($h^*=h/kT_c$, $L^*=L/b^{1/3}$).

Figure 1(a) depicts typical phase diagrams for the van der Waals fluid in the reservoir and inside pores with two different widths ($h^*=2.0$ for the systems depicted in this figure). As predicted by other models analogous to ours,[11,16] the critical point shifts to lower temperatures as L decreases, while the critical density passes through a maximum in the same process. At fixed wall separation L, the critical temperature decreases when the surface field h is increased, with the shift being stronger for the narrower pores.

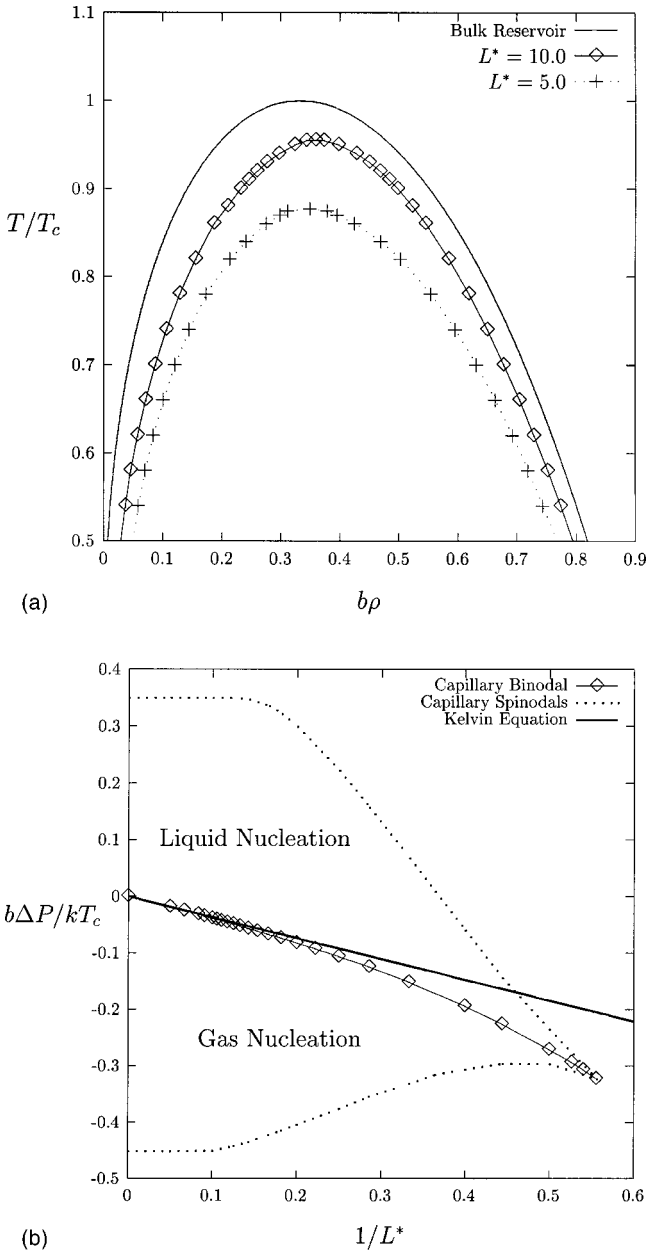

FIG. 1. (a) Phase diagram in the temperature–density plane for a van der Waals fluid in the bulk reservoir and in slit pores with $h^*=2.0$. The width of the pores is expressed in reduced units $L^*=L/b^{1/3}$. (b) Phase diagram in the $(\Delta P-1/L)$ plane for slit pores with surface field $h^*=2.0$ at a reduced temperature $T_r=T/T_c=0.5$. Predictions from the Kelvin equation are represented with a solid line ($\theta_o=74.83°$). The metastability region is delimited by the capillary spinodals (dotted lines).

The phase behavior of the system can also be studied by reducing the separation of the walls while maintaining a constant temperature. In this case, the reduction in the net amount of fluid–fluid interactions, combined with the stronger effect of the solid–fluid interactions, leads to the disappearance of the two-phase coexistence below a critical separation L_c. The corresponding phase diagram can be represented in a $(\Delta P-1/L)$ plane, with $\Delta P=P_l-P\approx\rho_l kT\ln(S)$ as a measure of the supersaturation. Capillary coexistence between a liquid and a gas configuration defines a binodal line in this type of phase diagram, as shown in Fig.

1(b) for the system with $h^*=2.0$ at a reduced temperature $T_r=0.5$ (corresponding to a bulk contact angle $\theta_o=74.83°$). The density profiles of the coexisting phases in this particular case correspond to an adsorbed gas-like phase $[\rho_o > \rho(L/2)]$ and a desorbed liquid-like phase $[\rho_o < \rho(L/2)]$. Results for the location of the liquid–vapor transition as predicted by Eq. (13) have also been included in this figure. In general, the predictions of the coexistence pressure using the Kelvin equation tend to be fairly accurate except for the smaller pores ($L^*<8$).

Dotted lines in Fig. 1(b) define the locus of the capillary spinodals for the system. In analogy to bulk fluids, capillary spinodals can be defined as the limit of metastability for liquid-like and gas-like inhomogeneous configurations inside the pore.[16,17] They delimit the regions where nucleation of droplets or bubbles determines the kinetics of phase separation in confined fluids. In our model, the location of the capillary spinodals is associated with regions where the grand potential excess has an inflection point as a function of the contact density ρ_o

$$(d^2\gamma/d\rho_o^2)=0, \tag{16}$$

with γ given by Eq. (5).

IV. HETEROGENEOUS NUCLEATION

Nucleation of droplets or bubbles in a metastable configuration inside the slit pore will occur on the walls of the system except for highly repulsive surface fields (drying conditions). Because of the symmetry of the walls and the surface potential $\Phi[\rho_o,\rho_L]$, critical nuclei in the system are expected to have cylindrical symmetry, with their density profiles depending on the distance perpendicular to one of the substrates (z) and on the radial distance (r) to the symmetry axis perpendicular to the walls.

Solutions to the Euler–Lagrange equation [Eq. (4)] representing critical nuclei in the open system correspond to saddle points of the grand potential in Eq. (1). The same solutions become minima of the Helmholtz free-energy $F=\Omega+\mu\rho$ when the total number of particles in the system N is fixed.[5,6] In this case, the system can be thought of as being contained inside a cylindrical container limited by the walls of the capillary and by a perfectly nonwetting–nondrying curved surface with a radius of curvature R much greater than the radius of the nucleus (the presence of this surface does not alter the distribution of matter in the system). The restriction

$$N=\int_{2\pi RL}\rho(\mathbf{r})d\mathbf{r}, \tag{17}$$

can be introduced into Eq. (4) to eliminate the dependence on the chemical potential μ. In particular, the chemical potential for the van der Waals fluid can be rewritten as[6]

$$\mu=KT\ln(N)-kT\ln\left(\int_{2\pi RL}d\mathbf{r}[1-b\rho(\mathbf{r})]\times e^{-[kTb\rho(\mathbf{r})/(1-b\rho(\mathbf{r}))-2a\rho(\mathbf{r})-K\nabla^2\rho(\mathbf{r})]/kT}\right). \tag{18}$$

The resulting Euler–Lagrange equation has the form

$$\frac{df[\rho(\mathbf{r})]}{d\rho(\mathbf{r})}-K\nabla^2\rho(\mathbf{r})=kT\ln(N)-kT\ln\left(\int_{2\pi RL}d\mathbf{r}[1-b\rho(\mathbf{r})]\times e^{-[kTb\rho(\mathbf{r})/(1-b\rho(\mathbf{r}))-2a\rho(\mathbf{r})-K\nabla^2\rho(\mathbf{r})]/kT}\right), \tag{19}$$

which can be solved by a nonlinear multigrid method for given values of N and T.[18] Additional boundary conditions should also be satisfied

$$K(d\rho/dz)_{z=0}=-h_o-g_o\rho_o,\qquad K(d\rho/dz)_{z=L}=h_L+g_L\rho_L, \tag{20a}$$

$$(d\rho/dr)_{r=0}=0. \tag{20b}$$

The work of formation of the critical nucleus with a density profile $\rho(r,z)$ is then given by the grand potential difference

$$\Delta\omega^*=\Omega[\rho(r,z)]-\Omega[\rho_\alpha(z)], \tag{21}$$

where $\Omega[\rho_\alpha(z)]$ is the grand potential of the surrounding metastable phase with density $\rho_\alpha(z)$ inside the capillary. The thermodynamic properties of this phase can be obtained once the chemical potential of the system μ is evaluated through Eq. (18).

We have followed the properties of critical nuclei inside pores of different widths as a function of the supersaturation S. Figure 2(a) shows the evolution of the work of formation $\Delta\Omega^*$ for a system with $h^*=2.0$ and $L^*=8.0$ at $T_r=0.5$. The height of the barrier to nucleation diverges at the thermodynamic condition for capillary coexistence ($S=0.8809$ for this case) and goes to zero at the capillary spinodal ($S=2.496$). For $S<1$, where capillary condensation occurs inside the pore but the vapor is the stable phase in the bulk, the structure of the critical nucleus is always that of a liquid tube connecting the two plates of the capillary; we present a typical density profile for this kind of nucleus in Fig. 3(a). As the supersaturation is increased, the size of the cluster decreases and starts getting thinner in its middle section [Fig. 3(b)], until it finally breaks into two pieces for thermodynamic states close to the spinodal.

For states with $S>1$, condensation inside the capillary is favored over condensation in the bulk for slit pores with attractive and even moderately repulsive walls. For these supersaturated vapors, however, competition between condensation via a liquid tube and via the formation of a single droplet attached to only one of the walls of the slit pore may occur at high supersaturations. In wide pores, there is always a range of values of the supersaturation where two different types of nuclei can be found [Fig. 2(a)]. Heterogeneous nucleation via a single droplet is favored close to the spinodal and down to a value of S where liquid-like densities are reached at the center of the capillary. Under such conditions, nucleation of the new phase should likely proceed by means of the formation of a droplet on a wall as suggested by recent molecular dynamics simulations.[2] The crossover between the barrier to nucleation via a single droplet or via a liquid tube

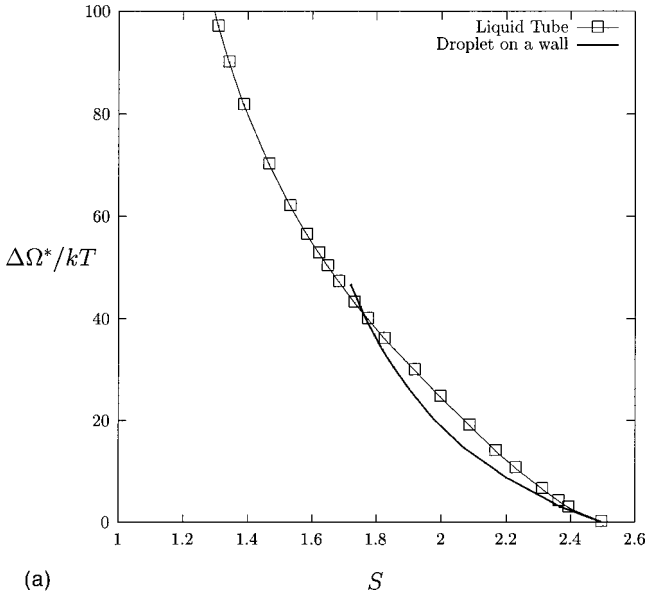

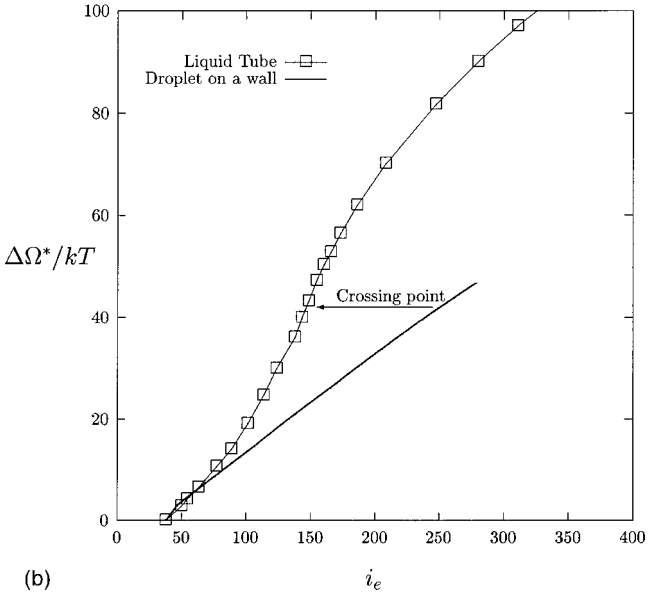

FIG. 2. Work of formation $\Delta\Omega^*$ of critical clusters (liquid tubes and droplets on a wall) in a slit pore: $L^*=8.0$, $h^*=2.0$, $T_r=0.5$, as a function of (a) supersaturation S; (b) size i_e. The arrow in (b) points out the size difference between the two types of clusters at the point of intersection of their corresponding energy barriers in (a).

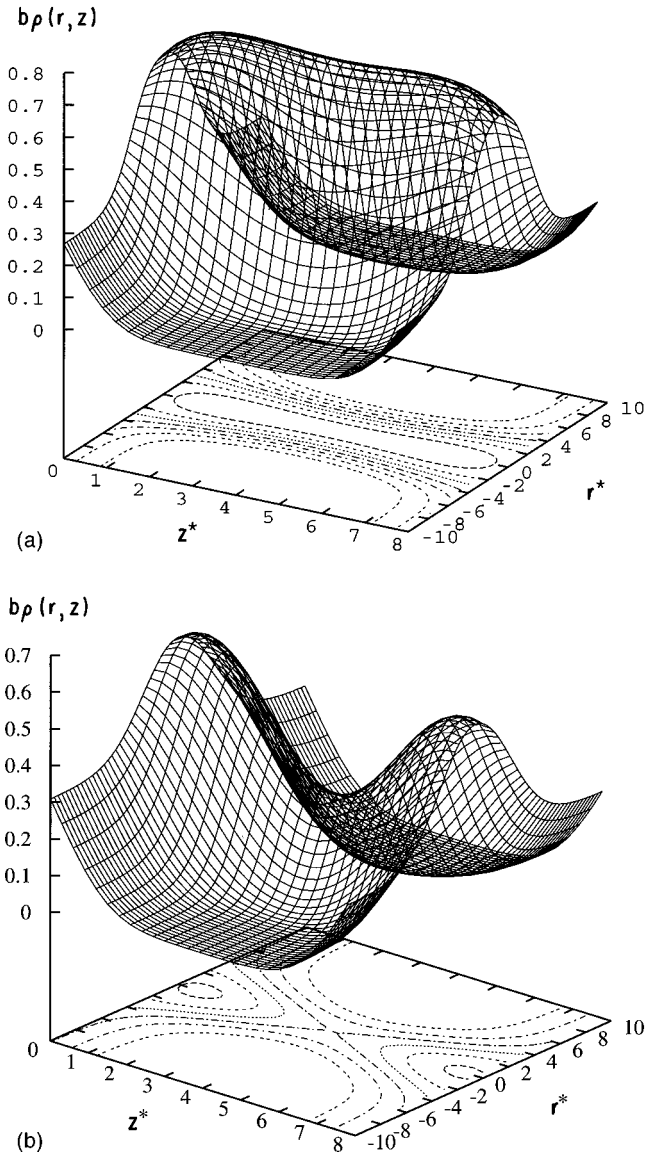

FIG. 3. Density profiles $\rho(r,z)$ for critical liquid tubes in a slit pore with $L^*=8.0$ and $h^*=2.0$ at $T_r=0.5$. (a) $S=1.60$, $\Delta\Omega^*/kT=55.55$, $i_e=169.0$; (b) $S=2.16$, $\Delta\Omega^*/kT=17.50$, $i_e=101.0$. Contours of constant density are shown as projections on the $(r^*=r/b^{1/3}, z^*=z/b^{1/3})$ plane.

occurs for values of S for which the height of the critical droplet measured perpendicular to the wall is still considerably smaller than the width of the pore L^*. For lower supersaturations, nucleation proceeds through the formation of a liquid bridge between the capillary walls.

For most supersaturations, the size of the two types of clusters that can form inside the capillary, as measured by the clusters' excess number of particles

$$i_e=\int_{2\pi RL} d\mathbf{r}(\rho(x,z)-\rho_\alpha(z)), \tag{22}$$

is very different. The single droplet solution tends to be much bigger than the liquid tube except very close to the capillary spinodal. Results for the work of formation of the critical clusters as a function of their size i_e in a slit pore with $L^*=8.0$ are shown in Fig. 2(b).

For systems in which the value of the surface field h favors partial wetting $(0<\theta_o\leqslant\pi/2)$, the work of formation of the critical tubes decreases with decreasing wall separation L at a given supersaturation, as illustrated in Fig. 4 for the fluid with $h^*=2.0$ (where we have also included, for comparison, results for the work of formation of a droplet adsorbed to a single wall, and the energy barrier for homogeneous nucleation in the reservoir fluid). For the wider pores, critical clusters corresponding to a single droplet on a wall do not exist for supersaturations much lower than that at the intersection with the energy barrier for the critical liquid tubes. As the width of the pore decreases, the capillary binodal and spinodal shift to lower supersaturations and there is a critical value of L below which the energy barriers for

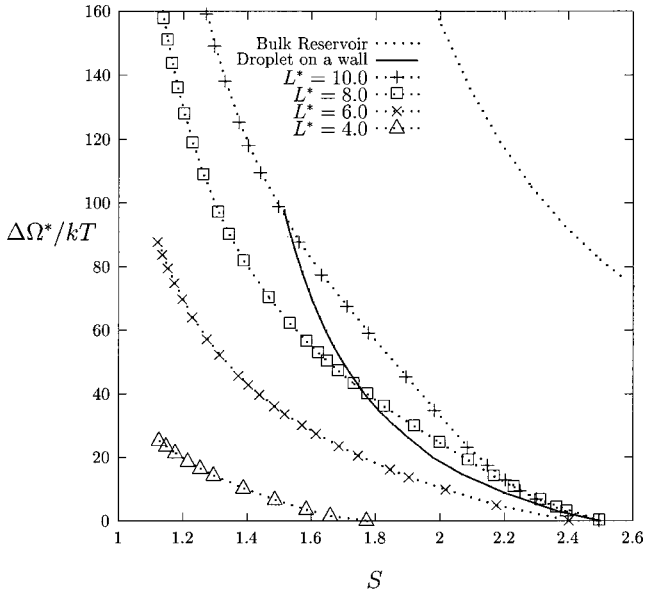

FIG. 4. Work of formation $\Delta\Omega^*$ of critical clusters (liquid tubes and single droplet on a wall) as a function of the supersaturation S^* for slit pores of various widths L^* ($h^*=2.0$, $T_r=0.5$). The energy barrier for homogeneous nucleation in the bulk fluid is included in this figure (dotted line).

nucleation of the liquid tube and the single droplet do not intersect any longer. For pores narrower than the critical one, the liquid tube becomes the preferred path for nucleation of the stable phase inside the capillary at all supersaturations.

When the interactions of the fluid with the walls of the capillary are such that partial drying is favored ($\pi/2<\theta_o<\pi$), the energy barrier for nucleation inside the slit pore starts increasing as the width decreases, particularly for the smaller pores at low supersaturations (see Fig. 5 for a system

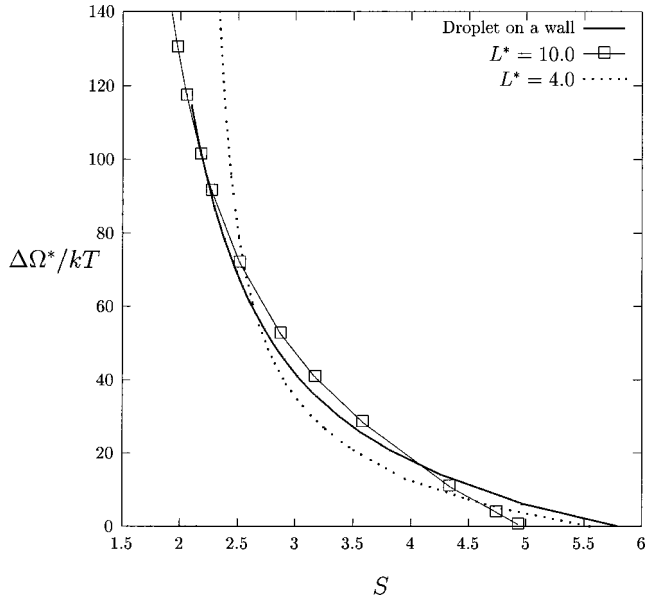

FIG. 5. Work of formation $\Delta\Omega^*$ of critical clusters (liquid tubes and single droplet on a wall) as a function of the supersaturation S for slit pores with two different widths ($h^*=0.5$, $T_r=0.5$). Results for the case of the single droplet on a wall should only be compared to those of a slit pore with $L^*=10.0$; for the narrower pore, this type of cluster only exists over a very limited range of supersaturations (very close to the spinodal).

with $h^*=0.5$, corresponding to a bulk contact angle $\theta_o=132.41°$). In this type of pore, the energy difference at a given S between the barrier to nucleation of the liquid tube and the droplet in contact with one wall tends to be smaller than the one observed under partial wetting conditions. For these more repulsive pores, the tube-like critical cluster does not thin out in its middle section at high supersaturations but starts detaching from the walls. Close to the spinodal the work of formation of a ''free'' critical cluster in the middle of the pore becomes smaller than the energy cost of forming a droplet on one of the walls (see Fig. 5).

We have also explored the properties of critical bubbles formed in metastable liquids inside slit pores of various widths. Analogous results to those just described apply to this kind of system, where critical bubbles that resemble vapor tubes connecting the two plates take the place of the liquid bridges, as supported by recent computer simulations.[3] The behavior of critical bubbles (tube-like and adsorbed on one wall) under partial wetting (partial drying) conditions qualitatively resembles that of critical droplets under partial drying (partial wetting) conditions.

V. CAPILLARITY APPROXIMATION

We will now compare our results to those generated by a simpler model based on the ''capillarity approximation'' (CA). The basic idea behind this model is to treat even the small nucleating clusters as if they were macroscopic droplets with surface tension. Suppose a droplet of liquid is in contact with one or two of the pore walls as well as with a metastable vapor at pressure P; the work of formation for this configuration [Eq. (21)] can be expressed as

$$\Delta\Omega = -V\Delta P + A_{lg}\gamma_{lg} + A_{sl}(\gamma_{sl}-\gamma_{sg}) + \tau L_{slg}, \tag{23}$$

where $\Delta P = P_l - P$ is the pressure difference between the liquid in the droplet and the surrounding vapor, V is the volume of the droplet, A_{lg} and A_{sl} are the areas of condensed phase in contact with the vapor and the substrates, respectively, and τ is the line tension of the three-phase contact line of length L_{slg}.

In the particular case of a single droplet in contact with one wall, the shape that minimizes the work of formation $\Delta\Omega$ is a spherical sector with a contact angle θ given by[19]

$$\gamma_{sl}-\gamma_{sg}+\gamma_{lv}\cos\theta+\frac{\tau}{R\sin\theta}=0. \tag{24}$$

The critical droplet that defines the barrier to nucleation has a radius $R=2\gamma_{lg}/\Delta P$, and the height of this barrier can be expressed as[19–21]

$$\Delta\Omega_{\mathrm{CA}}^{\mathrm{drop}}=\frac{16\pi\gamma_{lg}^3}{3(\Delta P)^2}f(\theta)+\frac{2\pi\tau\gamma_{lg}\sin\theta}{\Delta P}, \tag{25}$$

with

$$f(\theta)=\frac{(2+\cos\theta)(1-\cos\theta)^2}{4}. \tag{26}$$

For a critical liquid tube with cylindrical symmetry in contact with two identical walls at $z=0$ and $z=L$, the work

of formation can be expressed in terms of the position of the liquid–gas interface, $r(z)$, in the following form:[4]

$$\frac{\Delta\Omega[r(z)]}{2} = -\Delta P \pi \int_0^{L/2} r(z)^2 dz + 2\pi\gamma_{lg} \times \int_0^{L/2} r(z)(1+(dr(z)/dz)^2)^{1/2} dz + \pi r(0)^2(\gamma_{sl}-\gamma_{sg}) + 2\pi\tau r(0), \quad (27)$$

where $r(0)$ is the radius of the liquid bridge at contact with the walls. The shape of the critical nucleus can then be generated by solving the differential equation associated with the extremum $\delta\Delta\Omega[r(z)]/\delta r(z)=0$ under the boundary conditions

$$(dr(z)/dz)_{z=L/2}=0, \quad (28a)$$

$$\gamma_{sl}-\gamma_{sg}+\gamma_{lv}\cos\theta+\frac{\tau}{r(0)}=0, \quad (28b)$$

with $\cos\theta=\sin\theta(dr(z)/dz)_{z=0}$ and $[r(0)+r(L/2)]=2\gamma_{lg}/\Delta P$. The height of the barrier to nucleation for the liquid tube $\Delta\Omega_{\mathrm{CA}}^{\mathrm{tube}}$ can then be calculated by substituting the solution to the Euler–Lagrange equation $r(z)$ back into Eq. (27). For all practical purposes, the shape of the critical nucleus turns out to be very close to that of a meniscus with cylindrical symmetry and local curvature $\kappa=2/R$ (semicircular shape), where $R=L/(2\cos\theta)$ and θ is given by Eq. (28b). Hence, the explicit expressions for $\Delta\Omega_{\mathrm{CA}}^{\mathrm{tube}}$ and $r(0)$ that can be generated assuming a semicircular shape for any cross section of the critical tube are very accurate.

In order to compare the results of our density functional theory (DFT) with the predictions of the capillarity approximation for the van der Waals fluid, it is necessary to evaluate not only the different interfacial tensions $\gamma_{lg},\gamma_{sl},\gamma_{sg}$, for our model, but also the line tension τ associated with the three-phase contact line. When the coexisting liquid and gas phases in the bulk fluid are placed in contact with one substrate, the line tension τ in a partially wet state is given by[9]

$$\tau=\min_\rho \lim_{R_{ij}\to\infty}\int_{A_s} d\mathbf{a}\Omega[\rho(\mathbf{r})]-\sum_{i,j}\gamma_{ij}R_{ij}, \quad (29)$$

where the distances R_{ij} are the lengths of the three different two-phase interfaces within the area of integration. The area is chosen in a plane perpendicular to the three-phase contact line, with sides perpendicular to any intersecting two-phase interface.[22]

Figure 6 shows the results of our calculations for the work of formation of critical droplets inside a slit pore with $L^*=10.0$ and $h^*=2.0$ at $T_r=0.5$, using both DFT and CA. We include results for both types of clusters, liquid tube and single droplet on a wall, at different values of ΔP, taken as a measure of the supersaturation. The inclusion of the effect of the line tension on the work of formation of critical clusters seems to be crucial to generate reasonable predictions using CA (compare with the predicted barrier height when the line tension is assumed to be equal to zero in Fig. 6). The line tension for this particular system is negative, $\tau^*=\tau b^{1/3}/KT_c=-0.605$, but similar results have been obtained in systems with positive values of τ (e.g., $g=0$, $h>0$). As was the case in our study of heterogeneous nucleation on a flat wall with a short-ranged potential, the predictions of CA for partially wetted systems follow closely those of DFT at low supersaturations when the line tension contribution to the free energy is taken into account. However, the capillary approach becomes less accurate as one approaches the surface spinodals.

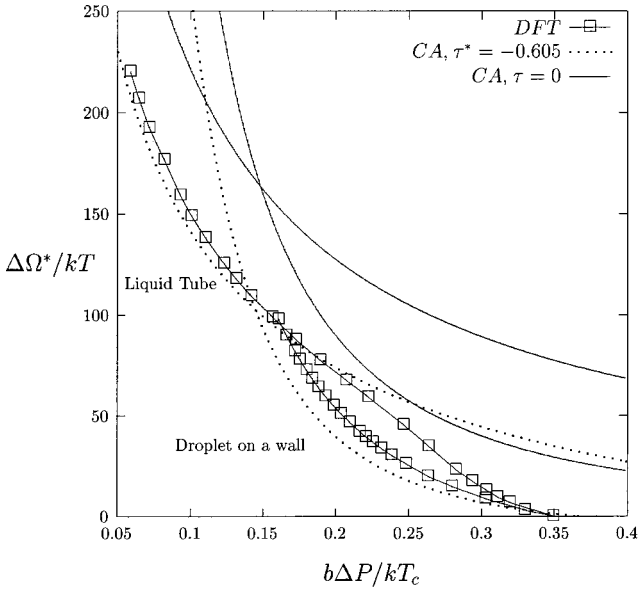

FIG. 6. Comparison of the work of formation $\Delta\Omega^*$ of critical clusters as predicted by the density functional theory (DFT) and the capillarity approximation (CA) at different supersaturations S ($L^*=10$, $h^*=2.0$, $T_r=0.5$). Results for the case when the line tension contribution to the free energy is not included in the calculations are also shown in this figure (solid lines).

The predictions of CA closely agree with those of DFT for different widths of the slit pore, as illustrated in Fig. 7(a) for a surface field $h^*=2.0$ ($\theta_o=74.83°$) at constant supersaturation ΔP. However, for systems with more repulsive walls, in which the work of formation of the critical tubes is not a monotonic increasing function of L, CA fails drastically [see Fig. 7(b), for the case $h^*=0.5$].

The results depicted in Figs. 7(a) and 7(b) can be used to determine the nature and magnitude of the additional solvation force between the walls associated with the formation of the critical cluster at a given supersaturation. In this case, the solvation force F_{solv} is given by

$$F_{\mathrm{solu}}=-d\Delta\Omega^*/dL. \quad (30)$$

In partially wetted pores the solvation force is always attractive and increases with the width of the pore at constant S or ΔP. In more drying capillaries, like the ones illustrated in Fig. 7(b), the force is only attractive ($F_{\mathrm{sol}}<0$) for the wider pores, as illustrated in Fig. 8 for a system with $h^*=0.5$. As we can see in this figure, the predictions for F_{solv} of CA are quantitatively different from those of DFT for all values of L (the better agreement with CA in the limit of $\tau=0$ is a mere coincidence for this particular case).

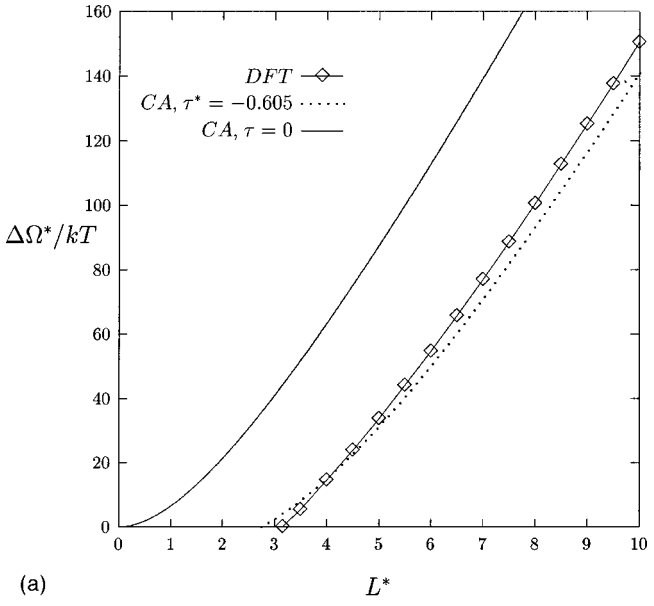

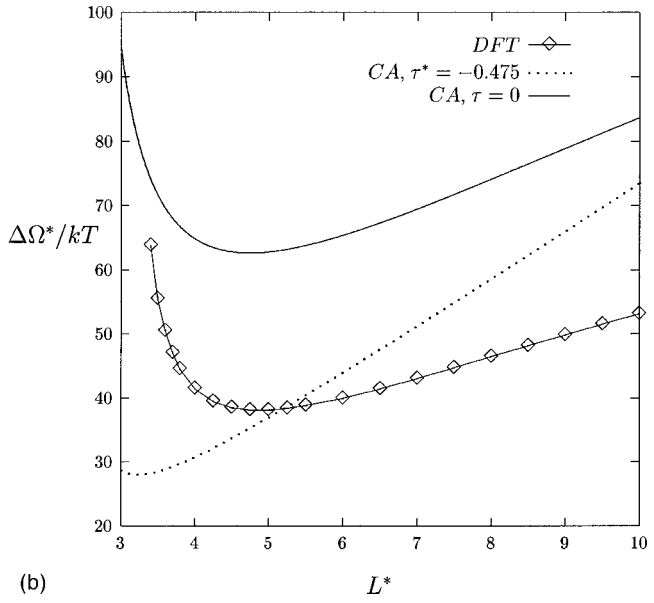

FIG. 7. (a) Comparison of the work of formation $\Delta\Omega^*$ of critical liquid tubes as predicted by DFT and CA at different pore widths L^* and constant supersaturation. (a) $h^*=2.0$, $\Delta bP/kT_c=0.1$; (b) $h^*=0.5$, $\Delta Pb/kT_c=0.4$.

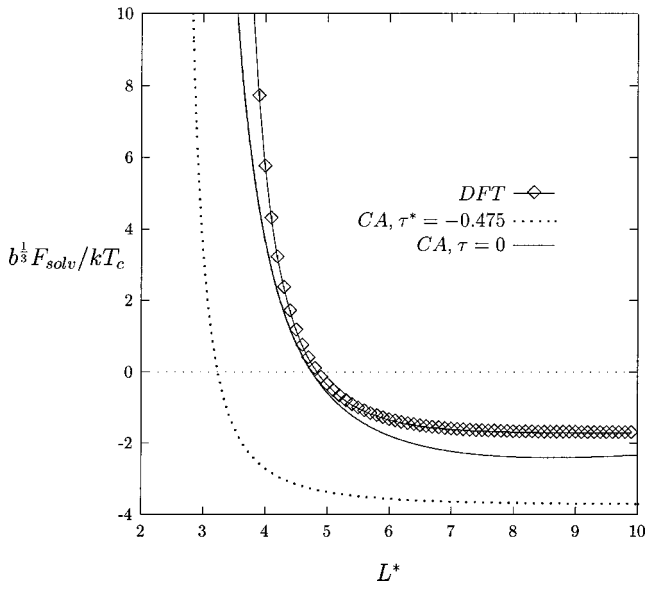

FIG. 8. Solvation force F_{solv} at different wall separations L^* for a surface field $h^*=0.5$ at $T_r=0.5$ and $\Delta Pb/kT_c=0.4$. The line tension of the bulk fluid in contact with a wall is negative, $\tau=-0.475$, in this case. Results for DFT and CA are included in this figure.

VI. DISCUSSION

Our density functional calculations predict a crossover between two nucleation mechanisms for condensation (or drying) transitions in slit pores. For large enough wall separations, nucleation occurs on one wall and the presence of the other is irrelevant; this limit reduces to the case of heterogeneous nucleation on a planar substrate. For small enough separations, however, the critical nucleus is a bridge connecting the two walls. We have shown that the capillarity approximation provides a reasonable qualitative account of most of our results, but only if the line tension is incorporated; more quantitative aspects are not predicted by this macroscopic theory.

One useful role for density functional theory is to suggest order parameters that can then be used in simulation-based approaches. The rarity of nucleation events under realistic conditions makes direct simulation difficult. The observational cluster method developed by Kusaka and co-workers[23] for simulation of nucleation uses configuration-biased umbrella sampling to explore states that would not often be seen in simple Monte Carlo simulations and thus to map out the nucleation path. A key ingredient is the selection of one or more order parameters, which emerge naturally from density functional theory, for biasing the Monte Carlo steps. A similar observation applies to the transition path sampling method of Bolhuis and Chandler.[3] For example, in the case of nucleation in a slit pore, where two different types of critical nuclei can be found for supersaturations $S>1$, the distinction between these two possible states could be established by using the difference in the fluid density at each wall as an appropriate order parameter (i.e., the difference would be zero for a symmetrical liquid tube, but not for a single droplet attached to one of the walls).

It will be interesting in the future to extend these calculations from slit pores to cylindrical pores. Because of the change in symmetry, the nature of the critical nucleus for condensation and evaporation will be quite different in this case. For a large enough cylindrical pore, the critical nucleus will be a cap on the inner surface of the pore, but for small pores it is not clear what the favored geometry will be. The nature of the critical nucleus and its free energy in the simple case of a single pore need to be understood before other aspects of capillary condensation that depend on fluid dynamics or pore topology can be explored. An additional direction that can be effectively studied with density functional theory is the nucleation of condensation and bubble formation for fluid mixtures in pores.

ACKNOWLEDGMENT

This work was supported by the National Science Foundation (Grant No. CHE 9800074).

[1] L. D. Gelb, K. E. Gubbins, R. Radhakrishnan, and M. Sliwinska-Bartkowiak, Rep. Prog. Phys. **62**, 1573 (1999).
[2] K. Yasuoka, G. T. Gao, and X. C. Zeng, J. Chem. Phys. **112**, 4279 (2000).
[3] P. G. Bolhuis and D. Chandler, J. Chem. Phys. **113**, 8154 (2000).
[4] F. Restagno, L. Bocquet, and T. Biben, Phys. Rev. Lett. **84**, 2433 (2000).
[5] V. Talanquer and D. W. Oxtoby, J. Chem. Phys. **100**, 5190 (1994).
[6] V. Talanquer and D. W. Oxtoby, J. Chem. Phys. **104**, 1483 (1996).
[7] J. W. Cahn, J. Chem. Phys. **66**, 3667 (1977).
[8] H. Nakanishi and M. E. Fisher, Phys. Rev. Lett. **49**, 1565 (1982).
[9] J. S. Rowlinson and B. Widom, *Molecular Theory of Capillarity* (Oxford University Press, New York, 1989).
[10] R. Evans, Adv. Phys. **28**, 143 (1979).
[11] H. Nakanishi and M. E. Fisher, J. Chem. Phys. **78**, 3279 (1983).
[12] U. Marini Bettolo Marconi, Phys. Rev. A **38**, 6267 (1988).
[13] D. E. Sullivan and M. M. Telo da Gama, in *Fluid Interfacial Phenomena*, edited by C. A. Croxton (Wiley, New York 1986).
[14] R. Evans, J. Phys.: Condens. Matter **2**, 8989 (1990).
[15] S. Dietrich, in *Phase Transitions and Critical Phenomena*, edited by C. Domb and J. L. Lebowitz (Academic, New York, 1988), Vol. 12.
[16] R. Evans, U. Marini Bettolo Marconi, and P. Tarazona, J. Chem. Phys. **84**, 2376 (1986).
[17] H. Nakanishi and P. Pincus, J. Chem. Phys. **79**, 997 (1983).
[18] W. H. Press, S. A. Teukolsky, W. T. Vetterling, and B. P. Flannery, *Numerical Recipes in* FORTRAN (Cambridge University Press, New York, 1992).
[19] G. Navascués and P. Tarazona, J. Chem. Phys. **75**, 2441 (1981).
[20] D. Turnbull, J. Chem. Phys. **18**, 198 (1950).
[21] R. D. Gretz, J. Chem. Phys. **45**, 3160 (1966).
[22] S. Perković, E. M. Blokhuis, and G. Han, J. Chem. Phys. **102**, 400 (1995).
[23] I. Kusaka, Z.-G. Wang, and J. H. Seinfeld, J. Chem. Phys. **108**, 3416 (1998); I. Kusaka, D. W. Oxtoby, and Z.-G. Wang, *ibid.* **111**, 9958 (1999).